



Cite this: *Chem. Sci.*, 2020, **11**, 7053

All publication charges for this article have been paid for by the Royal Society of Chemistry

Received 16th April 2020

Accepted 19th June 2020

DOI: 10.1039/d0sc02162h

rsc.li/chemical-science

Introduction

The concept of 1,3-dipolar cycloaddition (1,3-DC), pioneered by Huisgen in the 1960s,¹ has continued to influence a broad range of disciplines from medicine to materials sciences and even life sciences.² 1,3-DCs are reactions between a 1,3-dipole and a multiply bonded dipolarophile (e.g. alkenes, alkynes, carbonyls, and imines) to construct five-membered rings (Fig. 1a). This transformation represents one of the most effective approaches leading to synthetically and medicinally relevant five-membered heterocycles, and thus is pervasive in organic chemistry.³ However, the application of arenes as 2π -dipolarophiles in 1,3-DC reactions to produce fused heterocyclic scaffolds remains extremely challenging due to the substantial resonance stability of arenes. Although Huisgen showed that azomethine ylides are capable of undergoing 1,3-DC with dipolarophilic arenes as early as 1971,⁴ only activated arenes, such as heteroaromatic systems and nitro-substituted or fused arenes, are capable of engaging in such transformations.⁵

^aSchool of Chemistry and Chemical Engineering, Key Laboratory of Colloid and Interface Chemistry of Ministry of Education, Shandong University, Jinan 250100, P. R. China. E-mail: konglb@sdu.edu.cn

^bSchool of Materials Science & Engineering, PCFM Lab, Sun Yat-sen University, Guangzhou 510275, P. R. China. E-mail: kezhf3@mail.sysu.edu.cn

^cShenzhen Grubbs Institute and Department of Chemistry, Southern University of Science and Technology, Shenzhen 518055, P. R. China

^dState Key Laboratory of Elemento-Organic Chemistry, Nankai University, Tianjin 300071, P. R. China

† Electronic supplementary information (ESI) available. CCDC 1977878–1977884.

For ESI and crystallographic data in CIF or other electronic format see DOI: 10.1039/d0sc02162h

BNN-1,3-dipoles: isolation and intramolecular cycloaddition with unactivated arenes[†]

Rui Guo,^a Jingxing Jiang,^b Chenyang Hu,^c Liu Leo Liu,^b Ping Cui,^a Meihua Zhao,^a Zhuofeng Ke,^b*^b Chen-Ho Tung^b and Lingbing Kong^b*^{ad}

The mono-base-stabilized 1,2-diboranylidenehydrazine derivatives featuring a 1,3-dipolar BNN skeleton are obtained by dehydrobromination of $[\text{ArB}(\text{Br})\text{NH}]_2$ ($\text{Ar} = 2,6$ -diphenylphenyl (Dpp), $\text{Ar} = 2,6$ -bis(2,4,6-trimethylphenyl)phenyl (Dmp) or $\text{Ar} = 2,4,6$ -tri-*tert*-butylphenyl (Mes*)) with N-heterocyclic carbenes (NHCs). Depending on the Ar substituents, such species can be isolated as a crystalline solid ($\text{Ar} = \text{Mes}^*$) or generated as reactive intermediates undergoing spontaneous intramolecular aminoboration of the proximal arene rings via [3 + 2] cycloaddition ($\text{Ar} = \text{Dpp}$ or Dmp). The latter reactions showcase the 1,3-dipolar reactivity toward unactivated arenes at ambient temperature. In addition, double cycloaddition of the isolable BNN species with two CO_2 molecules affords a bicyclic species consisting of two fused five-membered BN_2CO rings. The electronic structures of these BNN species and the mechanisms of these cascade reactions are interrogated through density functional theory (DFT) calculations.

To date, only one set of examples describing intramolecular cycloadditions of azomethine ylides with unactivated arenes has been achieved, albeit under flash vacuum pyrolysis conditions.⁶

1,3-Dipoles, which feature a delocalized three-center 4π -electron system with a separation of charge over the three atoms (Fig. 1a), can be classified into two broadly defined categories according to the geometry of the central atom: propargyl/allenyl and allyl 1,3-dipoles.⁷ The generation of a variety of transient or persistent 1,3-dipoles consisting of carbon, nitrogen, oxygen, sulfur and phosphorus as well as their cycloaddition reactivities

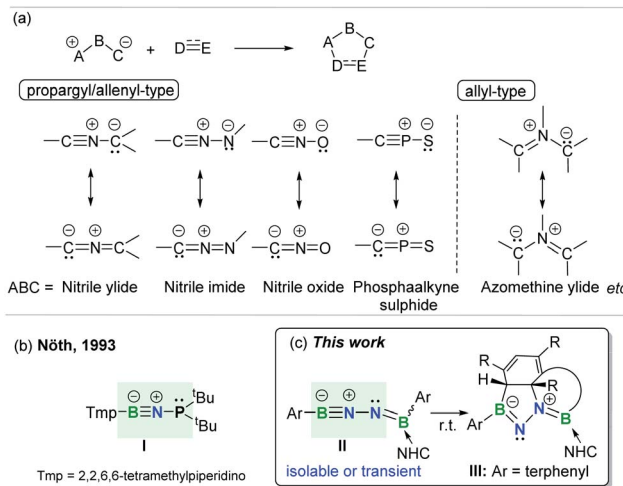


Fig. 1 (a) 1,3-Dipolar cycloaddition and representative 1,3-dipoles. (b) BNP-1,3-dipole. (c) This work.



have been extensively investigated over the past decades.⁷ However, boron-containing analogs of 1,3-dipoles are seldom encountered. To date, the only one example of a stable propargyl/allenyl-type BNP-1,3-dipole **I** was described by Nöth *et al.* in 1993 (Fig. 1b).⁸

Given the wide ranging applications of BN-containing heterocyclic compounds in organic synthesis, catalysis, materials science, and biomedical research, synthetic strategies toward a series of BN-scaffolds of azaborines, diazaboroles, diazadiborinines, triazadiboroles, and BN-polycyclic aromatic hydrocarbons *etc.* have been developed.⁹ For example, very recently, Kinjo and Ota described the synthesis of a neutral aromatic boron-rich inorganic benzene analog, namely 1,4-diaza-2,3,5,6-tetraborinine,¹⁰ while the group of Braunschweig synthesized complex BN-heterocycles *via* the reactions of organic azides with diaryl(dihalo)diboranes(4).¹¹ However, synthesis of fused BN-heterocyclic skeletons *via* 1,3-DC with unactivated arenes is hitherto unknown.¹² It is important to note that incorporation of heteroatoms into the 4π scaffold of 1,3-dipoles significantly effects the π -bond strength and frontier orbital energies,¹³ thereby modulating the ensuing reactivity. This prompted us to prepare and investigate reactions of an novel family of main group 1,3-dipoles containing a BNN-core. In the present work, we report the generation of mono-base-stabilized 1,2-diboranylidenehydrazines ArBNN(BNC)Ar **II** (Fig. 1c). Depending on the Ar substituents, such species can be isolated and characterized or generated *in situ* as reactive intermediates that spontaneously engage with the proximal unactivated arenes *via* intramolecular 1,3-DC to afford fused BN-heterocycles **III**.

Results and discussion

Cycloaddition reactivity of transient BNN-1,3-dipoles

In targeting a 1,2-diboranylidenehydrazine, we sought to incorporate abundant steric protection around boron to disfavor cyclooligomerization.¹⁴ Accordingly, we chose ArBBr₂ with a sterically encumbering 2,6-diphenylphenyl (Dpp) or 2,6-bis(2,4,6-trimethylphenyl)phenyl (Dmp) substituent (Scheme 1). The borylated hydrazines **1** (¹¹B NMR: 36.3 ppm) and **2** (¹¹B NMR: 32.4 ppm) were prepared in moderate yields *via* reactions of ArBBr₂ with bis(trimethylsilyl)hydrazine. The formulations of

1 and **2** as [DppB(Br)NH]₂ and [DmpB(Br)NH]₂, respectively, were unambiguously validated by high resolution mass spectrometry and X-ray diffraction studies (Fig. 2a and b). In the solid-state structures, the BN-involved-butadiene framework of **2** appears to be a *E,E*-configuration with a nearly coplanar B₂Br₂C₂N₂H₂ structure, whereas that of **1** is a formal *Z,Z*-configuration.

Noting that N-heterocyclic carbenes (NHCs) are potent Brønsted bases¹⁵ and ancillary ligands exhibiting excellent capability for stabilization of highly reactive main group species,¹⁶ we reacted **1** with 3 equivalents of 1,3-di-*tert*-butylimidazol-2-ylidene (I'Bu) in benzene at room temperature (Scheme 1). The dehydrobromination proceeded immediately with precipitation of [I'BuH][Br]. After recrystallization, a new species **3** was obtained as a yellow crystalline solid in 50% yield. The ¹¹B NMR spectrum of **3** revealed two broad singlets at 43.0 and 23.0 ppm, indicating the presence of two inequivalent tri-coordinate boron centers. The ¹H NMR spectrum displayed a multiplet resonance at 2.68 ppm and a doublet at 4.42 ppm, integrating for one proton each.

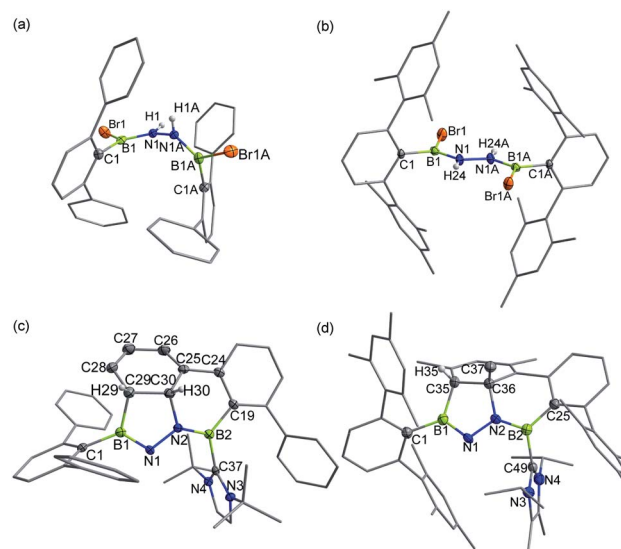
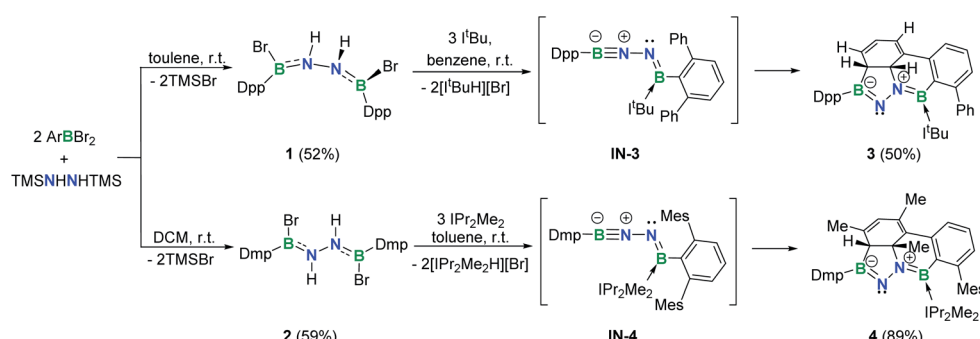


Fig. 2 Solid-state structures of **1** (a), **2** (b), **3** (c) and **4** (d). Hydrogen atoms except for N-H, C29-H, C30-H and C35-H are omitted for clarity. Thermal ellipsoids are set at the 30% probability level.



Scheme 1 Synthesis of **1–4** (Dpp = 2,6-diphenylphenyl; Dmp = 2,6-bis(2,4,6-trimethylphenyl)phenyl; Mes = 2,4,6-trimethylphenyl).



Single crystal X-ray diffraction revealed **3** to be a tetracyclic BN-embedded $3aH$ - $3a^1H$ -acephenanthrylene derivative, resulting from the apparent $[3 + 2]$ cycloaddition of a transient BNN-1,3-dipole **IN-3** across the proximal flanking phenyl substituent of Dpp moiety (Fig. 2c). The bond lengths of C25–C26 (1.350(3) Å) and C27–C28 (1.339(4) Å) are in the typical range of C=C double bonds, whereas those of C25–C30 (1.486(3) Å), C26–C27 (1.452(3) Å), C28–C29 (1.480(3) Å) and C29–C30 (1.543(3) Å) appear to be C–C single bonds. These structural parameters are in line with the formation of a 1,3-cyclohexadiene unit from an arene. Both the cyclohexadiene and BC_2N_2 rings are essentially planar (the sum of internal angles = 719.86° and 539.54° , respectively), and the torsion angle of B1–C29–C30–C25 is $123.43(17)^\circ$. The B1–N1 and B2–N2 bond lengths are 1.387(3) and 1.375(3) Å, respectively, are significantly shorter than those in **1** (1.444(7) Å, av.) and fall within the typical range of B=N double bonds in aminoboranes.¹⁷ Additionally, the N1–N2 bond distance of 1.4243(19) Å is marginally longer than that in **1** (1.391 (8) Å) and close to that reported for $[\text{Mes}_2\text{B}(\text{H})\text{N}]_2$ (1.411(4) Å).¹⁸ These structural parameters reveal a B=N–N=B skeleton. The B1–N1–N2–B2 torsion angle of $-171.37(18)^\circ$ suggests a near coplanarity. Atoms B1 and B2 bear sp^2 hybridization character, judging from the angular sums of 359.95° and 359.93°, respectively.

In an analogous fashion, treatment of **2** with 1,3-diisopropyl-4,5-dimethylimidazol-2-ylidene (IPr_2Me_2) in toluene led to a species **4** (^{11}B NMR: 41.3 and 22.3 ppm) (Scheme 1) with a fused tetracyclic framework (Fig. 2d). It is noteworthy that compounds **3** and **4** could also be prepared in the dark, which rules out a light-induced radical mechanism for this transformation.

Mechanistic studies

To gain more insight into the mechanism leading to **3**, density functional theory (DFT) calculations were carried out at the SMD-M06-2X/def2-TZVP//M06-2X/def2-SVP level of theory (Fig. 3a). While the double dehydrobromination of **1** with $\text{I}^{\prime}\text{Bu}$ followed by mono-ligation to generate **IN-3** is endergonic by 11.8 kcal mol⁻¹, the precipitation of $[\text{I}^{\prime}\text{BuH}][\text{Br}]$ over the course of the reaction promotes this conversion. Subsequently, the approach of the proximal phenyl group toward the BNN moiety in **IN-3** gives rise to **TS** (27.7 kcal mol⁻¹) in a concerted manner. Intrinsic bond orbital (IBO) calculations,¹⁹ which have been demonstrated to give an exact representation of any Kohn-Sham DFT wave function, showcase that the redistribution of π -electrons over the phenyl and BNN fragments forms B1–C29 and C30–N2 σ -bonds to furnish **3** (-2.9 kcal mol⁻¹) (Fig. 3a). The additional linkage (*i.e.*, C24–C25 or B2–C19 bonding) of **3** plays an essential role in stabilizing the dearomatized framework. In the absence of either the C24–C25 or B2–C19 linkage (Fig. 3b), the corresponding intermolecular 1,3-DC using model molecules is calculated to be endergonic by 14.1 or 8.1 kcal mol⁻¹, respectively. Collectively, these results demonstrate that the intramolecular 1,3-DC is exergonic and favorable whereas the formation of **3a** or **3b** in an intermolecular fashion is endergonic and unfavorable.

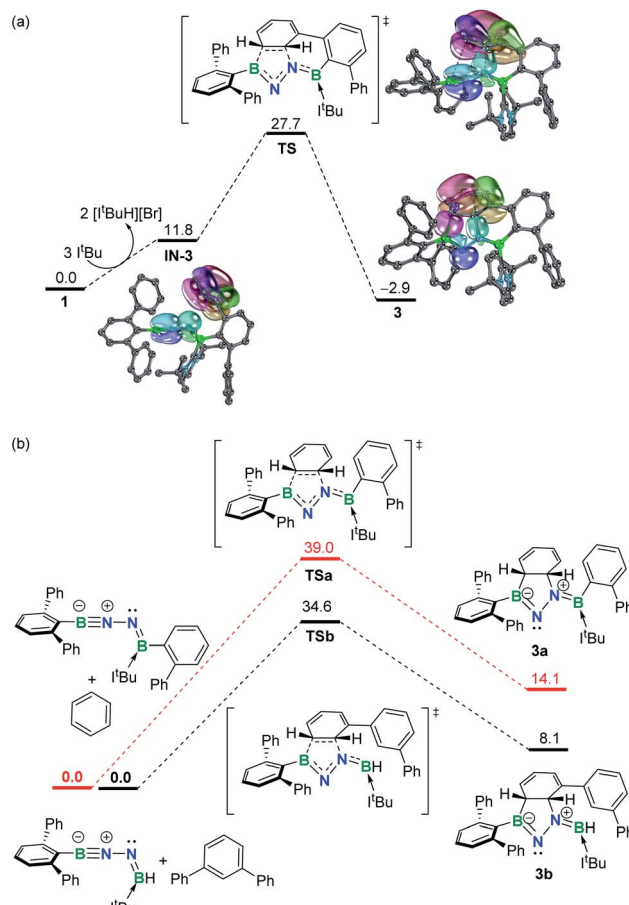


Fig. 3 (a) Free energy profile for formation of **3** with selected IBOs (75% of the orbital electron's density). (b) Free energy profiles for formation of **3a** and **3b**. Energies are given in kcal mol⁻¹.

The NHC coordination in **3** is also crucial for stabilization of the fused tetracycle, probably due to the compensation of the intrinsic electron deficiency of B2 and the enhancement of the nucleophilicity of N2. The absence of $\text{I}^{\prime}\text{Bu}$ is spontaneously destructive to the tetracyclic framework leading to the base-free 1,2-diboranylidenehydrazine DppB=N–N=BDpp upon an unrestricted geometry optimization.

It is important to note that the incorporation of heteroatoms into unsaturated organic skeletons forms multiply bonded main group species have proven particularly effective in enabling cycloadditions with arenes in the ground state.²⁰ For example, the Power and Tokitoh groups independently demonstrated intermolecular $[4 + 2]$ cycloadditions of transient dialumenes with benzene/toluene.²¹ Stephan and co-workers described a reversible intramolecular $[4 + 2]$ cycloaddition of a phosphaalkene to an arene ring.²² More recently, the group of Kinjo showed the diboration of a series of polycyclic aromatic hydrocarbons by a 1,3,2,5-diazadiborinine derivative.²³ The formation of **3** and **4** represents the first examples of dearomatic bifunctionalization of arenes *via* 1,3-dipolar cycloaddition under mild conditions, thus providing another avenue to access novel fused BN-heterocyclic scaffolds. In addition, such

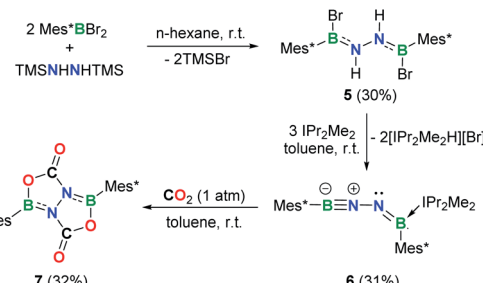


transformations are rare examples of unactivated arenes behaving as 2π components in cycloaddition reactions.^{6,20,23}

A stable BNN-1,3-dipole

Efforts to prevent the reaction of the BNN moiety toward sterically accessible arene substituents were undertaken. To this end, we prepared $[\text{Mes}^*\text{B}(\text{Br})\text{NH}]_2$ (**5**, $\text{Mes}^* = 2,4,6\text{-tri-}t\text{-butylphenyl}$) analogously to **1** and **2** (Fig. 4a). Reaction of **5** with 3 equivalents of IPr_2Me_2 in toluene afforded a yellow solution, from which species **6** was isolated in 31% yield after work-up (Scheme 2). In the ^{11}B NMR spectrum of **6**, two broad resonances at 33.7 and 2.8 ppm were observed. The former is considerably downfield shifted with respect to those of iminoborane–carbene adducts (12.6–24.0 ppm),²⁴ while the latter is comparable to the chemical shift seen for iminoborane, $\text{Mes}^*\text{B}\equiv\text{N}^t\text{Bu}$ (4.3 ppm).²⁵ The ^1H NMR spectrum of **6** in C_6D_6 showed one set of peaks assignable to the IPr_2Me_2 ligand and no evidence of N–H resonances.

Single crystals of **6** suitable for X-ray diffraction were obtained by slow evaporation of a concentrated *n*-hexane solution at $-25\text{ }^\circ\text{C}$ within 24 h. X-ray crystallography confirmed the structure as $\text{Mes}^*\text{B}\equiv\text{N}=\text{N}\equiv\text{B}(\text{IPr}_2\text{Me}_2)\text{Mes}^*$ (Fig. 4b). While such a linear BNN moiety is reminiscent of recent works of main group diazo and N_2 chemistry by the Stephan²⁶ and Braunschweig²⁷ groups, respectively, compound **6** contains a BNNB motif in which one of the boron atoms is only dicoordinate. In a related work, Klingebiel *et al.* disclosed that the iminoborane supported by two bis(trimethylsilyl)amido groups could easily self-cyclize through C–H addition across the $\text{B}\equiv\text{N}$ bond.²⁸ The most prominent structural feature is the nearly linear C1–B1–



Scheme 2 Synthesis of **5–7** ($\text{Mes}^* = 2,4,6\text{-tri-}t\text{-butylphenyl}$).

N1–N2 chain ($\angle \text{C1–B1–N1} = 176.0(2)^\circ$; $\angle \text{B1–N1–N2} = 169.24(19)^\circ$) with the B1–N1 bond length of $1.236(4)$ Å that is almost same to that observed for $\text{Mes}^*\text{B}\equiv\text{N}^t\text{Bu}$ ($1.232(6)$ Å).²⁵ The N1, N2, B2, C7, C37 atoms are in a planar arrangement (mean deviation from plane = 0.0081 Å). The B2–N2 bond ($1.368(3)$ Å) appears at lengths seen for carbene-stabilized iminoborane complexes ($1.304(3)$ – $1.360(5)$ Å).²⁴ The N1–N2 bond distance of $1.351(2)$ Å is significantly longer in comparison with that in the dinitrogen bis(borylene) compound $\{[(\text{CAAC})\text{DurB}]_2(\mu_2\text{-N}_2)\}$ ($1.248(4)$ Å).²⁷ Nevertheless, this N1–N2 bond length is markedly shorter than that in **5** ($1.396(4)$ Å), indicating the enhanced interaction between these two unsaturated BN fragments in **6**. The geometry of the B2=N2 bond adopts a formal *E*-configuration, similar to iminoborane-CAAC adducts (CAAC = cyclic (alkyl)(amino)carbene), reported by Braunschweig, Bertrand, Stephan *et al.*^{24b–d} The presence of a hydrogen bonding interaction of $\text{N}(2)\cdots\text{H}(43)\text{–C}(43)$ ($D = 2.9482(1)$ Å, $\theta = 137.947(4)^\circ$) is identified in the solid state. Collectively, the dipolar BNN fragment features a propargyl/allenyl-like structure. Compound **6** represents the first example of a room-temperature-stable BNN-1,3-dipole.

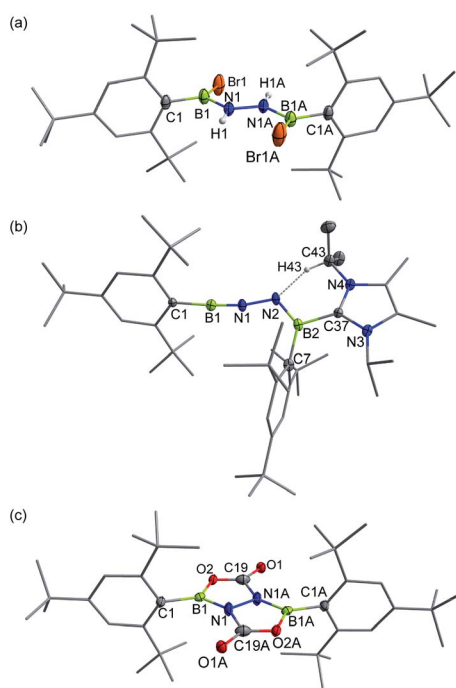


Fig. 4 Solid-state structures of **5** (a), **6** (b) and **7** (c). Hydrogen atoms except for N–H and C43–H are omitted for clarity. Thermal ellipsoids are set at the 30% probability level.

Bonding

The electronic properties of **6** were further investigated based on DFT calculations using the M06-2X/def2-SVP optimized structure. The LUMO and LUMO + 1 predominantly involves the π^* -antibonding interaction, which is delocalized over one of the Mes^* rings, B1–N1 and B2–N2 bonds, and the imidazole ring (Fig. 5a and b). The HOMO is the out-of-plane B1–N1 and B2–N2 π orbitals (Fig. 5c), whereas the in-plane B1–N1 π orbital as well as a lone pair of electrons on N2 are represented by the HOMO – 1 (Fig. 5d). Furthermore, the Wiberg bond indices (WBIs) of the B1–N1, N1–N2 and B2–N2 bonds from the natural bond orbital (NBO) calculations (M06-2X/TZVP) are 1.87, 1.14 and 1.35, respectively (Table S2†), suggesting that the NHC ligation on B2 remarkably diminishes the π -donation from N2 to B2. To gain more insight into the interaction between two unsaturated BN fragments, the second-order perturbation theory of the NBO method was applied, which shows a strong hyperconjugative delocalization from the p-type N2 lone pair to the B1–N1 π^* -antibonding orbital with a donor–acceptor stabilization energy of $20.2\text{ kcal mol}^{-1}$ (Fig. S33†). The partial double bond character of N1–N2 is further evidenced by natural localized molecular



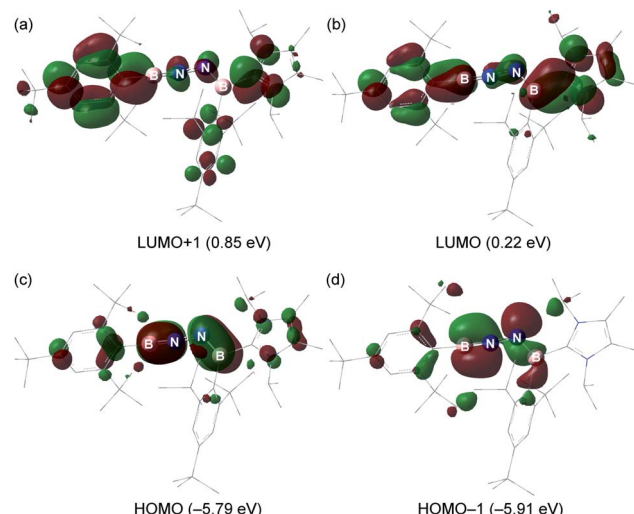


Fig. 5 (a–d) Key molecular orbitals of **6** (isovalue = 0.03, calculated at the M06-2X/Def2-SVP level of theory).

orbital (NLMO) analysis that reveals a highly delocalized N2 lone pair toward N1 (Fig. S33†). The B1 (0.82) and B2 (0.73) atoms are positively charged, while N1 (−0.65) and N2 (−0.72) atoms carry negative charges (Table S3†). Bending the B–N–N angle up to 155° from 172° in **6** has negligible energetic cost (2.7 kcal mol^{−1}), indicating a flexibility of the molecule along this coordinate.

Compound **6** exhibits an absorption maximum in the UV/Vis spectrum in *n*-hexane at 372.3 nm (*f* = 0.7601) (Fig. S28†). This absorption was primarily attributed to the π–π* transitions (HOMO – 1 → LUMO and HOMO → LUMO) according to TD-DFT calculations (Fig. S34†).

Natural resonance theory (NRT) calculations (M06-2X/TZVP) on the simplified model **6'** shows that two leading propargyl-type forms **6'a** (24.4%) and **6'b** (22.5%) (Fig. 6a), coupled with several other propargyl-type forms (weights <5%; Fig. S35†), predominately contribute to the electronic structure of this BNN-1,3-dipole. Two allenyl-type forms **6'c** (2.2%) and **6'd** (2.1%) are identified with low weights (Fig. 6a). It is noteworthy

that NHCs have been shown to feature a carbon–nitrogen multiple bond based on NRT analysis.²⁹ In contrast, the nitrile ylide $\text{CH}_3\text{CNC}(\text{CH}_3)_2$ shows an opposite trend with propargyl-type form weight of 16.5% and allenyl-type form weight of 66.1% (Fig. 6b). This finding provides hints that substitution of C atoms with heteroatoms is capable of shifting electronic properties.

Reactivity of **6** toward CO_2

As a further probe of the 1,3-dipole ability of **6**, we examined its reactivity toward carbon dioxide (CO_2) (Scheme 2). Exposure of a toluene solution of **6** to 1 atm dry CO_2 at room temperature for 5 min resulted in a slight yellow cloudy solution. After work-up, colorless crystals of **7** (¹¹B NMR: 36.0 ppm) were isolated in 32% yield. The presence of a carbonyl carbon is evidenced by a resonance at 155.5 ppm in the ¹³C NMR spectrum. An unambiguous elucidation of the structure of **7** was performed based on single crystal X-ray diffraction (Fig. 4c), revealing a system containing a fused bicyclic B,N,O-involved heterocycle. Interestingly, two CO_2 molecules were fixed *via* a double 1,3-DC, concurrent with the loss of IPr_2Me_2 . It is important to mention that sequential CO_2 cycloaddition by BN species to construct a fused bicyclic compound is hitherto unknown, although **I** ([3 + 2] cycloaddition),⁸ iminoboranes ([2 + 2] cycloaddition)^{14b,24b} and a series of N/B based frustrated Lewis pairs (FLPs)^{30,31} for CO_2 activation have been explored.

Conclusions

More than six decades after Huisgen's classification of 1,3-dipoles, this work demonstrates that a BNN-1,3-dipole, namely a mono-base-stabilized 1,2-diboraneylidenehydrazine **6**, is synthetically achievable. Single crystal X-ray diffraction in combination with DFT calculations provide insights into the most plausible electronic structure of **6**, which features a conjugated BN chain with a formal $\text{B}_1\equiv\text{N}_1$ triple bond and a $\text{B}_2=\text{N}_2$ double bond. Remarkably, in the presence of a sterically accessible flanking arene substituent, the corresponding BNN-1,3-dipoles are highly fleeting and susceptible to [3 + 2] cycloaddition reactions, affording BN-containing fused tetra-cycles **3** and **4**. Such 1,3-dipolar reactivity is also reflected by the 1,3-DC of **6** with CO_2 to give **7**. Further reactivity investigations of such BNN-1,3-dipoles, as well as the synthesis of their constitutional isomers, are currently underway in our laboratory.

Conflicts of interest

The authors declare no competing financial interests.

Acknowledgements

We gratefully acknowledge financial support from the Natural Science Foundation of China (Grants 21971144, 21702228 and 21673301), the Natural Science Foundation of Shandong Province (Grants ZR2019ZD46 and ZR2017MB021), the Key R&D

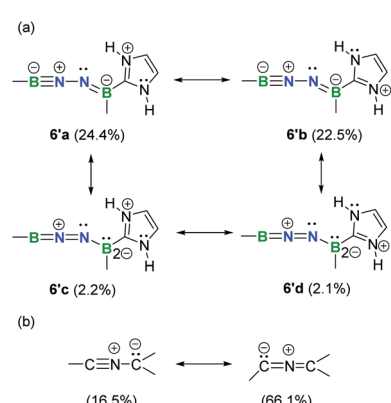


Fig. 6 Selected predominant resonance structures and their weights for **6'** (a) and nitrile ylide $\text{CH}_3\text{CNC}(\text{CH}_3)_2$ (b).



Program of Shandong Province (Grant 2019GGX102032), the Guangdong Natural Science Funds for Distinguished Young Scholars (Grant 2015A030306027), the Qilu Youth Scholar Funding of Shandong University (Grant 11190088963021), the Multidisciplinary Research and Innovation Team of Young Scholars of Shandong University (Grant 2020QNQT007) and the Fundamental Research Funds for the Central Universities. L. L. L. gratefully acknowledge the start-up fund of SUSTech. The DFT calculations were made possible by the facilities of the Shared Hierarchical Academic Research Computing Network (SHARCNET: <http://www.Sharcnet.ca>) and Compute Canada. L. L. L. thanks Prof. D. W. Stephan (U of T) and Prof. J. Zhu (XMU) for kindly providing access to computational facilities. L. L. L. thanks Dr E. A. Romero at the University of California, Berkeley and Dr R. Wei (SINAP) for valuable discussion. We thank Prof. D. Sun (SDU) and Dr Y. Li (NTU) for assistance with the X-ray crystal structure analysis. We thank the reviewers for their valuable suggestions.

Notes and references

- (a) R. Huisgen, *Angew. Chem., Int. Ed. Engl.*, 1963, **2**, 633–645; (b) R. Huisgen, *Angew. Chem., Int. Ed. Engl.*, 1963, **2**, 565–598; (c) R. Huisgen, *Proc. Chem. Soc.*, 1961, 357–396; (d) R. Huisgen, *Festschrift der Zehnjahresfeier des Fonds der Chemischen Industrie*, Düsseldorf, 1960, p. 73.
- (a) N. Nishiwaki, *Methods and Applications of Cycloaddition Reactions in Organic Synthesis*, Wiley-VCH, Weinheim, Germany, 2014; (b) Synthetic Applications of 1,3-Dipolar Cycloaddition Chemistry Toward Heterocycles and Natural Products, in *The Chemistry of Heterocyclic Compounds*, ed. A. Padwa and W. H. Pearson, Wiley, New York, NY, USA, 2003, vol. 59.
- (a) L.-J. Wang and Y. Tang, Intermolecular 1,3-dipolar cycloadditions of alkenes, alkynes and allenes, in *Comprehensive Organic Synthesis*, ed. P. Knochel and G. A. Molander, Elsevier, Amsterdam, The Netherlands, 2nd edn, 2014, vol. 4, pp. 1342–1383; (b) R. S. Menon and V. Nair, Intramolecular 1,3-dipolar cycloadditions of alkenes, alkynes and allenes, in *Comprehensive Organic Synthesis*, ed. P. Knochel and G. A. Molander, Elsevier, Amsterdam, The Netherlands, 2nd edn, 2014, vol. 4, pp. 1281–1341.
- R. Huisgen and W. Scheer, *Tetrahedron Lett.*, 1971, **12**, 481–484.
- J. H. Ryan, *Arkivoc*, 2015, **1**, 160–183.
- B. R. Henke, A. J. Kouklis and C. H. Heathcock, *J. Org. Chem.*, 1992, **57**, 7056–7066.
- R. Huisgen, *J. Org. Chem.*, 1976, **41**, 403–419.
- J. Kröner, H. Nöth, K. Polborn, H. Stolpmann, M. Tacke and M. Thomann, *Chem. Ber.*, 1993, **126**, 1995–2002.
- (a) C. R. McConnell and S.-Y. Liu, *Chem. Soc. Rev.*, 2019, **48**, 3436–3453; (b) Z. X. Giustra and S.-Y. Liu, *J. Am. Chem. Soc.*, 2018, **140**, 1184–1194; (c) G. Bélanger-Chabot, H. Braunschweig and D. K. Roy, *Eur. J. Inorg. Chem.*, 2017, 4353–4368; (d) B. Su and R. Kinjo, *Synthesis*, 2017, **49**, 2985–3034; (e) P. G. Campbell, A. J. V. Marwitz and S.-Y. Liu, *Angew. Chem., Int. Ed.*, 2012, **51**, 6074–6092; (f) M. J. D. Bosdet and W. E. Piers, *Can. J. Chem.*, 2009, **87**, 8–29.
- K. Ota and R. Kinjo, *Angew. Chem., Int. Ed.*, 2020, **59**, 6572–6575.
- (a) D. Prieschl, G. Bélanger-Chabot, X. Guo, M. Dietz, M. Müller, I. Krummenacher, Z. Lin and H. Braunschweig, *J. Am. Chem. Soc.*, 2020, **142**, 1065–1076.
- (a) M. Schäfer, J. Schäfer, R. D. Dewhurst, W. C. Ewing, M. Krahfuß, M. W. Kuntze-Fechner, M. Wehner, C. Lambert and H. Braunschweig, *Chem.-Eur. J.*, 2016, **22**, 8603–8609; (b) H. Braunschweig, K. Geetharani, J. O. C. Jimenez-Halla and M. Schäfer, *Angew. Chem., Int. Ed.*, 2014, **53**, 3500–3504; (c) H. Braunschweig, A. Damme, J. O. C. Jimenez-Halla, B. Pfaffinger, K. Radacki and J. Wolf, *Angew. Chem., Int. Ed.*, 2012, **51**, 10034–10037.
- (a) L. Zhao, S. Pan, N. Holzmann, P. Schwerdtfeger and G. Frenking, *Chem. Rev.*, 2019, **119**, 8781–8845; (b) R. C. Fischer and P. P. Power, *Chem. Rev.*, 2010, **110**, 3877–3923.
- (a) M. Nutz, B. Borthakur, R. D. Dewhurst, A. Deissenberger, T. Dellermann, M. Schäfer, I. Krummenacher, A. K. Phukan and H. Braunschweig, *Angew. Chem., Int. Ed.*, 2017, **56**, 7975–7979; (b) L. Xie, J. Zhang, H. Hu and C. Cui, *Organometallics*, 2013, **32**, 6875–6878; (c) B. Kröckert, K.-H. van Bonn and P. Paetzold, *Z. Anorg. Allg. Chem.*, 2005, **631**, 866–868; (d) M. Geschwendtner, G. Elter and A. Meller, *Z. Anorg. Allg. Chem.*, 1993, **619**, 1474–1478; (e) P. Paetzold, *Adv. Inorg. Chem.*, 1987, **31**, 123–170.
- (a) P. Cui, R. Guo, L. Kong and C. Cui, *Inorg. Chem.*, 2020, **59**, 5261–5265; (b) R. Guo, X. Huang, M. Zhao, Y. Lei, Z. Ke and L. Kong, *Inorg. Chem.*, 2019, **58**, 13370–13375; (c) Y. Wang, H. Hu, J. Zhang and C. Cui, *Angew. Chem., Int. Ed.*, 2011, **50**, 2816–2819; (d) H. Cui and C. Cui, *Chem.-Asian J.*, 2011, **6**, 1138–1141; (e) Y. Gao, J. Zhang, H. Hu and C. Cui, *Organometallics*, 2010, **29**, 3063–3065; (f) H. Cui, Y. Shao, X. Li, L. Kong and C. Cui, *Organometallics*, 2009, **28**, 5191–5195; (g) R. S. Ghadwal, H. W. Roesky, S. Merkel, J. Henn and D. Stalke, *Angew. Chem., Int. Ed.*, 2009, **48**, 5683–5686.
- (a) V. Nesterov, D. Reiter, P. Bag, P. Frisch, R. Holzner, A. Porzelt and S. Inoue, *Chem. Rev.*, 2018, **118**, 9678–9842; (b) T. W. Hudnall, R. A. Ugarte and T. A. Perera, *N-Heterocyclic Carbenes: From Laboratory Curiosities to Efficient Synthetic Tools (2)*, The Royal Society of Chemistry, UK, 2017, pp. 178–237; (c) L. J. Murphy, K. N. Robertson, J. D. Masuda and J. A. C. Clyburne, *N-Heterocyclic Carbenes*, Wiley-VCH Verlag GmbH & Co. KGaA, New York, 2014, pp. 427–498; (d) E. Rivard, in *Comprehensive Inorganic Chemistry II*, ed. K. Poepelmeier, Elsevier, Amsterdam, 2013, pp. 457–484.
- K.-A. Østby, G. Gundersen, A. Haaland and H. Nöth, *Dalton Trans.*, 2005, 2284–2291.
- D. C. Pestana and P. P. Power, *Inorg. Chem.*, 1991, **30**, 528–535.
- (a) G. Knizia and J. E. M. N. Klein, *Angew. Chem., Int. Ed.*, 2015, **54**, 5518–5522; (b) G. Knizia, *J. Chem. Theory Comput.*, 2013, **9**, 4834–4843.



20 For low-valent main group species for arene activation, see: (a) A. Hermann, M. Arrowsmith, D. E. Trujillo-Gonzalez, J. O. C. Jimenez-Halla, A. Vargas and H. Braunschweig, *J. Am. Chem. Soc.*, 2020, **142**, 5562–5567; (b) J. Hicks, P. Vasko, J. M. Goicoechea and S. Aldridge, *J. Am. Chem. Soc.*, 2019, **141**, 11000–11003; (c) L. Zhu, J. Zhang and C. Cui, *Inorg. Chem.*, 2019, **58**, 12007–12010; (d) L. L. Liu, L. L. Cao, J. Zhou and D. W. Stephan, *Angew. Chem., Int. Ed.*, 2019, **58**, 273–277; (e) L. L. Liu, J. Zhou, L. L. Cao, R. Andrews, R. L. Falconer, C. A. Russell and D. W. Stephan, *J. Am. Chem. Soc.*, 2018, **140**, 147–150; (f) D. Wendel, A. Porzelt, F. A. D. Herz, D. Sarkar, C. Jandl, S. Inoue and B. Rieger, *J. Am. Chem. Soc.*, 2017, **139**, 8134–8137; (g) P. Bissinger, H. Braunschweig, K. Kraft and T. Kupfer, *Angew. Chem., Int. Ed.*, 2011, **50**, 4704–4707. For cyclobutadiene for arene cycloaddition, see: (h) Y. Inagaki, M. Nakamoto and A. Sekiguchi, *Nat. Commun.*, 2014, **5**, 3018–3023. For carboryne for arene cycloaddition, see: (i) D. Zhao, J. Zhang and Z. Xie, *Angew. Chem., Int. Ed.*, 2014, **53**, 8488–8491.

21 (a) R. J. Wright, A. D. Phillips and P. P. Power, *J. Am. Chem. Soc.*, 2003, **125**, 10784–10785; (b) T. Agou, K. Nagata and N. Tokitoh, *Angew. Chem., Int. Ed.*, 2013, **52**, 10818–10821.

22 L. L. Liu, J. Zhou, L. L. Cao, Y. Kim and D. W. Stephan, *J. Am. Chem. Soc.*, 2019, **141**, 8083–8087.

23 Y. Su, D. C. H. Do, Y. Li and R. Kinjo, *J. Am. Chem. Soc.*, 2019, **141**, 13729–13733.

24 (a) L. Winner, A. Hermann, G. Bélanger-Chabot, O. F. González-Belman, J. O. C. Jiménez-Halla, H. Kelch and H. Braunschweig, *Chem. Commun.*, 2018, **54**, 8210–8213; (b) F. Dahcheh, D. W. Stephan and G. Bertrand, *Chem.-Eur. J.*, 2015, **21**, 199–204; (c) F. Dahcheh, D. Martin, D. W. Stephan and G. Bertrand, *Angew. Chem., Int. Ed.*, 2014, **53**, 13159–13163; (d) H. Braunschweig, W. C. Ewing, K. Geetharani and M. Schäfer, *Angew. Chem., Int. Ed.*, 2015, **54**, 1662–1665.

25 G. Elter, M. Neuhaus, A. Meller and D. Schmidt-Bäse, *J. Organomet. Chem.*, 1990, **381**, 299–313.

26 (a) D. Zhu, Z.-W. Qu and D. W. Stephan, *Dalton Trans.*, 2020, **49**, 901–910; (b) L. L. Cao, J. Zhou, Z.-W. Qu and D. W. Stephan, *Angew. Chem., Int. Ed.*, 2019, **58**, 18487–18491; (c) C. Tang, Q. Liang, A. R. Jupp, T. C. Johnstone, R. C. Neu, D. Song, S. Grimme and D. W. Stephan, *Angew. Chem., Int. Ed.*, 2017, **56**, 16588–16592. See also: (d) R. L. Melen and D. W. Stephan, *Dalton Trans.*, 2015, **44**, 5045–5048.

27 (a) M.-A. Légaré, G. Bélanger-Chabot, R. D. Dewhurst, E. Welz, I. Krummenacher, B. Engels and H. Braunschweig, *Science*, 2018, **359**, 896–900; (b) M.-A. Légaré, M. Rang, G. Bélanger-Chabot, J. I. Schweizer, I. Krummenacher, R. Bertermann, M. Arrowsmith, M. C. Holthausen and H. Braunschweig, *Science*, 2019, **363**, 1329–1332.

28 K. Bode, U. Klingebiel, M. Noltemeyer and H. Witte-Abel, *Z. Anorg. Allg. Chem.*, 1995, **621**, 500–505.

29 L. Liu, D. A. Ruiz, D. Munz and G. Bertrand, *Chem.*, 2016, **1**, 147–153.

30 (a) A. R. Jupp and D. W. Stephan, *Trends Chem.*, 2019, **1**, 35–48; (b) D. W. Stephan, *Science*, 2016, **354**, aaf7229.

31 (a) B. R. Barnett, C. E. Moore, A. L. Rheingold and J. S. Figueroa, *Chem. Commun.*, 2015, **51**, 541–544; (b) Z. Lu, Y. Wang, J. Liu, Y. Lin, Z. H. Li and H. Wang, *Organometallics*, 2013, **32**, 6753–6758; (c) T. Voss, T. Mahdi, E. Otten, R. Fröhlich, G. Kehr, D. W. Stephan and G. Erker, *Organometallics*, 2012, **31**, 2367–2378; (d) M. A. Dureen and D. W. Stephan, *J. Am. Chem. Soc.*, 2010, **132**, 13559–13568.

